Molecular complexity and gene expression controlling cell turnover during a digestive cycle of carnivorous sponge Lycopodina hypogea

Emilie Le Goff, Camille Martinand-Mari, Khalid Belkhir, Jean Vacelet, Sabine Nidelet, Nelly Godefroy, Stephen Baghdiguian

Molecular complexity and gene expression controlling cell turnover during a digestive cycle of carnivorous sponge Lycopodina hypogea.

Emilie Le Goff[1], Camille Martinand-Mari[1], Khalid Belkhir[1], Jean Vacelet[2], Sabine Nidelet[3], Nelly Godefroy[1] *, Stephen Baghdiguian[1] *

[1] ISEM, CNRS, EPHE, IRD, Univ Montpellier, Montpellier, France

[2] IMBE, CNRS, IRD, Station Marine d'Endoume, Univ Aix-Marseille, Univ Avignon, 13007 [20]10 Marseille, France

[3] Montpellier GenomiX, Univ Montpellier, CNRS, INSERM, Montpellier France (New affectation : CBGP, INRA, CIRAD, IRD, Montpellier SupAgro, Univ Montpellier, Montpellier, France)

*Co-last and co-corresponding authors (nelly.godefroy@umontpellier.fr ; stephen.baghdiguian@umontpellier.fr)

Abstract

Lycopodina hypogea is a carnivorous sponge that tolerates laboratory husbandry very well. During a digestion cycle, performed without any digestive cavity, this species undergoes spectacular morphological changes leading to a total regression of long filaments that ensure the capture of prey and their reformation at the end of the cycle. This phenomenon is a unique opportunity to analyze the molecular and cellular determinants that ensure digestion in the sister group of all other metazoans. Using differential transcriptomic analysis coupled with cell biology studies of proliferation, differentiation, and programmed cell deaths (i.e., autophagy and the destructive/constructive function of apoptosis), we demonstrate that the molecular and cellular actors that ensure digestive homeostasis in a sister group of all remaining animals are similar in variety and complexity to those controlling tissue homeostasis in higher vertebrates. During a digestion cycle, most of these actors are finely tuned in a coordinated manner. Our data benefits from complementary approaches coupling in silico and cell biology studies and demonstrate that the nutritive function is provided by the coordination of molecular network that impacts the cells turnover in the entire organism.

Key words: Carnivorous sponge, Homeostasis, Metazoa morphogenesis, Cell biology, Transcriptomic analysis

Introduction

Although there is still some debate as to whether sponges or ctenophores are the sister group to all other metazoans, recent data seem to favor sponges as the ones with this phylogenetic position (Redmond and McLysaght 2021). Ctenophores possess a centralized ingestion/digestion system and nervous components (Dunn et al., 2015), which is not the case for sponges which present a large number of choanocytic chambers located throughout the entire body ensuring filtration and are devoid of any nervous system and digestive organ. A surprising point is that some sponges of the Cladorhizidae family, generally localized in the deep sea, have been able to drastically modify their strategy and organization as filter feeders by becoming carnivorous, discarding the unique aquiferous system of the Porifera but keeping the mobile and plastic comportment of the cells (Vacelet and Boury-Esnault 1995). Interestingly, an intermediate situation exists in some sponges of the *Chondrocladia* genus that retain the aquifer system while becoming carnivorous (Godefroy et al. 2019; Kübler and Barthel 1999). In this case, no study shows that the aquifer system still has a role in nutrition. Carnivorous sponges are an unusual example of metazoans digesting macro-preys without any digestive cavity such as acoels, xenacoelomorphs, and Platyhelminthes (Gavilán et al. 2019). Despite this evolutive innovation and simplified organization compared to higher metazoans, the cell fate is governed through the three fundamental cellular functions, i.e. proliferation, differentiation and programmed cell death (PCD), which are landmarks of metazoan homeostasis (Martinand-Mari et al. 2012).

In order to identify the molecular actors that control these cellular functions at the root of metazoans, we took advantage of the biological features of the carnivorous sponge *Lycopodina hypogea* (Vacelet and Boury-Esnault 1996) which, despite absence of any digestive cavity, digests macro-prey through the individual phagocytic action of cells. This process, which is exceptional in metazoans, implies unusual morphological modifications, involving first an organized migration due to a trophic migration of cells from all parts of the sponge toward the prey and then a reorganization. In *L. hypogea*, starved animals are characterized by many elongated filaments, which are crucial for the capture of prey. The filaments are attached to a structure that we call “apical ovoid body”. This structure surmounts a peduncle attached to the rock (Fig. 1). After capture, and during the digestion process, these filaments actively regress before being regenerated during a subsequent period of starvation (Godefroy et al. 2019; Martinand-Mari et al. 2012; Vacelet and Duport 2004).

To accomplish its functions, the sponge undergoes prey-induced filament resorption, carried out by apoptosis and active migration of cells with phagocytic activities toward the prey, and then filament reformation by the production and migration of new sclerocytes and other cell types. In the adult sponge, the two processes are in balance, maintaining a constant, “homeostatically” controlled amount, and size of filament between two successive cycles of digestion. This fact, as well as the histological observation that filament resorption is followed by filament reformation, led to the hypothesis that the two processes are mechanistically ‘‘coupled’’ to ensure global homeostasis of digestive functions. However, the identity of the cellular pathways and genes allowing this morphological homeostatic coupling during a digestion cycle (i.e., the capacity to return to the initial shape) remained unknown.

We hypothesize that digestion in *Lycopodina* requires, in addition to the genes directly involved in digestion (nucleases, lipases, glycosidases, proteases, etc.), the coordinated contribution of genes involved in cell turnover,

since cells must migrate towards food, while it is the opposite in most other metazoans. To test this hypothesis, we sequenced the transcriptomes of *Lycopodina hypogea* subjected to a strict 2-month experimental starvation or at various stages of a digestive cycle after experimentally controlled feeding and compared their transcript contents on the basis of this experimental design. Genes encoding stem cell markers and proteins implicated in cell cycle control, phagocytosis, autophagy, and apoptosis were specifically examined. Cell biology study was then conducted on the status of aforementioned mechanisms in order to correlate the variations of gene expression with cellular changes. This approach has the additional advantage of localizing the regions in which the mechanisms are activated at the level of the whole organism. To summarize, we made use of the *Lycopodina hypogea* model to analyze the molecular determinants that control the digestion cycle in a multicellular animal belonging to the suspected most ancestral metazoan groups (Simion et al. 2017).

Material and methods

Animal husbandry

Specimens of *Lycopodina hypogea* (Vacelet and Boury-Esnault 1996) were collected in the 3PP cave near La Ciotat on the Mediterranean coast of France (Vacelet 1996). The animals were transferred to small seawater tanks, 0.5–2 L, in the laboratory where they were kept in a dark chamber at a temperature of 13 °C. Under these conditions, the sponge can thrive for years, with a monthly water change and feeding with living *Artemia* nauplii.

mRNA isolation and sequencing

For each condition, two biological replicates were collected either after a 2-month starvation period (unfed control, 0 h) or 15 h, 40 h, and 216 h after feeding with *Artemia*. Total RNA was isolated with a RNeasy kit according to the supplier's instructions (QIAGEN). mRNA library of each individual was run for 100 bp, paired-end, read sequencing in an Illumina HiSeq2000 sequencer by the Montpellier MGX sequencing platform (http://www.mgx.cnrs.fr/).

Database analysis

Most bioinformatics analyses were performed by the MBB platform in Montpellier (http://mbb.univ-montp2.fr/). For each condition (2 months of starvation, 15 h, 40 h, or 216 h after feeding), cDNA libraries (with a mean insertion size of 1081 bp) were generated in duplicate (individuals A and B in Fig. 2e and Supplementary Information SI 1). To overcome the lack of reference transcriptome for *L. hypogea*, cleaned reads from the eight individuals were de novo assembled into contigs using Trinity transcriptome assembly software. The cleaning step consisted in removing sequences of *Artemia franciscana* (used to feed sponge) and sequences of *Ciona intestinalis* (another biological model currently used in our lab). For this step, we mapped reads using bowtie2 on a reference file made by concatenating *Artemia* transcriptome coming from a parallel project of our institute (PopPhyl ANR project) and *Ciona* sequences (from Ensembl). Only paired-end reads that failed to align (using –very-sensitive-local option) were retained. Bacterial sequences had no impact because the cDNA library was made with oligo-dTs targeting only eukaryotic mRNAs. Sequences from *L. hypogea* were extracted from these databases by TBLASTN

alignments with protein sequences of stem cell markers, cell cycle regulators, phagocytosis, autophagy, and apoptosis mechanisms from other model organisms (human, *Drosophila*, and nematode for all mechanisms). Yeast sequences were also used for autophagy since yeast is the most studied model for this cellular mechanism. Protein sequences from reference species were found on Uniprot (http://www.uniprot.org/) or Ensembl (http://www.ensembl.org/) websites. The *Lycopodina hypogea* isolated sequences were scanned with InterProScan 5 (https:// www.ebi.ac.uk/interpro/search/sequence-search) to verify the presence of functional or structural domains specific of each protein. In parallel, each selected sequence was used to conduct TBLASTN searches on NCBI (all databases) to name the sequence. When several incomplete sequences had the same best hit, we aligned them on this best hit sequence to see if some of them overlap. In this case, concerned sequences were considered as fragments of the same sequence, and we were used to reconstitute the entire sequence. Sequences too short and without specific domains were automatically discarded to avoid false positives. Then, the best assembly contigs were used as a reference for aligning reads from the 8 different individuals to estimate the expression levels (Bowtie, RSEM). From these normalized expression levels, appropriate statistical methods (Edger, Imb) were applied to identify genes whose expression levels vary significantly between conditions (X4), to identify molecular networks mainly involved in the morphological changes caused by nutrition cycling.

Detail protein sequences found by these analyses are listed in Supplementary Information SI 2 to SI 6.

For all mechanisms, we search with blast on NCBI database presence/absence of all studied genes in *Amphimedon queenslandica* genome. For autophagy, we added *Capsaspora owczarzaki* and *Monosiga brevicollis* (Supplementary Information SI 7 to SI 11).

TUNEL staining and indirect immunofluorescence analysis

Sponges were fixed for 30 min with 3.7% paraformaldehyde in filtered seawater and then permeabilized for 20 min at room temperature with 0.2% Triton X-100 in TS buffer (150 mM NaCl, 25 mM Tris, pH 7.5). TUNEL (transferase dUTP nick end labeling) staining (Merck, In Situ Cell Death Rhodamine Detection Kit, 12,156,792,910) was performed according to the manufacturer's instructions. In brief, sponges were incubated in TUNEL reaction mixture (enzyme solution 10% in label solution) for 1 h at 37 °C. Sponge, incubated for 30 min at 37 °C with DNase I recombinant purified from bovine pancreas (Merck, 04,536,282,001) prior to the TUNEL reaction, was used as positive control. Sponge, incubated without the enzyme solution during the TUNEL reaction, was used as negative control.

Fixed and permeabilized sponges were subjected to indirect immunofluorescence with rabbit anti-human MAPLC3 polyclonal antibodies (Santa Cruz Biotechnology, sc-28266: 1/100 in Tris-buffered saline buffer for 2 h at room temperature) as described previously (Le Goff et al. 2015; Martinand-Mari et al. 2012). Blocking steps were performed with Tris Saline (TS) buffer containing 1% bovine serum albumin (BSA). Samples were incubated with an appropriate secondary antibody, FITC-conjugated donkey-anti-rabbit immunoglobulins (Jackson Laboratories, 711–095-152: 1/50 in Tris Saline buffer), and DAPI (Euromedex, 1050A: 1/1000 of 1 mg/mL stock solution) for 1 h in the dark at room temperature. After washing, the samples were embedded in Dako fluorescence mounting medium (Dako, S3023). Specimens were analyzed with a Leica TCS-SPE laser confocal microscope (Montpellier RIO Imaging platform, France).

Apoptosis inhibition with ZVAD-FMK

ZVAD-FMK (Sigma V116) was added just before the feeding of sponges in seawater at a final concentration of 10 µM (stock solution: 100 mM in DMSO storage −20 °C), and then an addition was made every 24 h at the same concentration. A dimethyl sulfoxide (DMSO) control was performed under the same conditions. Sponges were then treated for TUNEL staining (see above).

EdU incorporation

EdU (5-ethynyl-2'-deoxyuridine) (Invitrogen, Click-iT EdU Imaging kit Alexa 488) was used as an alternative to bromodeoxyuridine (BrdU) labeling (see Martinand-Mari et al. 2012). Sponges were incubated for 24 h at 13 °C in seawater containing 50 µmol/L EdU and then fixed for 30 min with 3.7% paraformaldehyde and permeabilized for 20 min at room temperature with 0.2% Triton X-100 in TS buffer (150 mM NaCl, 25 mM Tris, pH 7.5). EdU detection was performed according to the manufacturer's instructions. Specimens were analyzed with a Leica TCS-SPE laser confocal microscope (Montpellier RIO Imaging platform).

TUNEL or EdU-positive nuclei counting

We counted the percentage of TUNEL or EdU-positive nuclei from DAPI/TUNEL/EdU z-stack-stained images obtained using a Leica SPE confocal microscope at the DBS-Optique MRI facilities (Montpellier, France) with ImageJ software. For each condition, the number of nuclei was counted in three independent experiments.

Statistical analysis

We used prop.test in R software (R Foundation for Statistical Computing) to compare percentage of positive TUNEL or EdU nuclei among sponges that were unfed, 15, 40, or 216 h post-nutrition. A first analysis with prop.test confirmed the homogeneity of $n = 3$ for each condition. Then, a second analysis tested the significance of the values for the comparisons between the different conditions.

Histology and cytology

The sponges were fixed after starvation or after feeding with *Artemia* nauplii. The fixation was performed at room temperature in 2.5% glutaraldehyde in a buffer composed of 0.4 $mol.l^{-1}$ sodium cacodylate/seawater (1/1) for 24 h. The sponges were then post-fixed in 2% osmium tetroxide in seawater for 2 h and de-silicified in 5% hydrofluoric acid for 30 min. They were then embedded in Araldite for light and transmission electron microscopy. Semi-thin Sections (0.5 µm) were stained with toluidine blue and were observed under a Leica DMLB microscope.

Results

The nutrition cycle is associated with substantial morphological modifications and a change in gene expression

As illustrated in Fig. 2a–d, *Lycopodina hypogea* is subject to morphological changes during the different stages of its nutrition cycle. Unfed animals are characterized by the presence of numerous elongated filaments (Fig. 2a).

After capture of a prey, the filaments actively regress, including those which were not involved in the capture. The prey is engulfed within a few hours by sponge cells coming from filaments and from other parts of the sponge body. While the large nuclei (white arrow head in the insert) belong to the prey (*Artemia* nauplii whose outline has been added in orange dotted line), the small ones which are difficult to distinguish at this magnification belong to the sponge (Fig. 2b). Forty hours after capture, the contour of the prey can no longer be distinguished because digestion is well advanced (Fig. 2c). After digestion, a subsequent period of starvation induces an important body remodeling with the growth of new filaments, returning the animal to its initial morphological state (shape homeostasis) (Fig. 2d). At this stage, large nuclei are barely visible, meaning the prey was almost completely digested.

To decipher the relationship between the phenotypic and molecular changes associated with the morpho-nutritional transition in *L. hypogea*, we performed a comparative transcriptomic study over a complete digestion cycle. A total of 230,000 contigs were rendered, for which a measured level of expression was available under the different conditions. The transcription levels of approximately 2% of all contigs (representing 4364 genes) were found to be positively or negatively regulated (> fourfold) with morpho-nutritional status. Figure 2e shows the expression profile of the regulated genes during the nutrition cycle. Gene expression changes radically after digestion (at 15 h and 40 h post-feeding). The more the digestion process progresses, the closer the gene expression profile is to that of fasting individuals (9 days versus 2-month starvation) without returning to the basal levels. This is in accordance with the presence of Artemia nuclei in the sponge body 9 days after feeding (Vacelet and Duport 2004 and data not shown).

Identification of molecular networks that control tissue homeostasis

To overcome the lack of *L. hypogea* sequenced genome, we generated a de novo transcriptome from the eight sequenced studied individuals and identified among all generated sequences, the ones corresponding to the proteins involved in shape regulation and tissue homeostasis. According to sponge cell plasticity, we first searched for stem cell markers. Three core pluripotency factors, *Oct4*, *Sox2*, and *Nanog*, have been introduced as essential factors for the maintenance of pluripotency and self-renewal of mammalian stem cells (Chambers and Tomlinson 2009; Kashyap et al. 2009). We did not find homologs of *Oct4* and *Nanog* in *L. hypogea* but found six members of the Sox family: *Sox B1a* to *c*, *Sox B2* and *Sox F* (Table 1 –red column “cellular identity and stem cell markers”). *Musashi* and *Piwi*, described in active stem cells in sponge were found in *Lycopodina* (Funayama 2013; Funayama et al. 2010; Okamoto et al. 2012).

By definition, stem cells have the ability to self-replicate and give birth to more than one mature daughter cell type. In sponges, two stem cell lineages have been described: the archaeocytes and choanocytes (not present in *Lycopodina*) (Ereskovsky 2018; Funayama 2013; Rinkevich et al. 2022) can self-renew and differentiate into various cell types. We searched for classical markers of identity of pinacocytes (epithelial-like cells), myocytes (contractile cells), or sclerocytes (skeletal cells) and found each of them (Table 1 – red column “cellular identity and stem cell markers”).

The regulation of shape in demosponges has a particular additional constraint; in the presence of a siliceous skeleton produced by sclerocytes, we sought to list the polymerization/depolymerization regulators of this skeleton present in the transcriptome of *Lycopodina hypogea*. All of them were found: *silicatein*, *silintaphin*, and

galectin for the polymerization and the stabilization of silicate filaments and the *silicase* for their degradation (Müller et al. 2014; Wang et al. 2012) (Table 1 – red column; transcripts in orange).

Next, we searched for transcripts involved in cell cycle regulation (*cyclins*, *cyclin-dependent-kinases (cdk)*, and their regulators). We found 12 *Cdk* and 17 *cyclins, E2F, DP,* and *Rb* but no *cyclin-dependent kinase inhibitors* (CDKN). Transcripts encoding proteins that interact with cyclin-Cdk complexes to block their kinase activity (for review, see Lim and Kaldis 2013) are apparently absent in *Lycopodina* (Table 1 – purple column "cell cycle control").

As cells need to respond to changes in nutrient availability to maintain metabolic homeostasis and viability, we also looked for autophagic transcripts and markers of phagocytosis. Autophagy is one of the main cellular responses to nutrient removal, and phagocytosis regulates the clearance of pathogens and cell debris (e.g., damaged cells) necessary to tissue homeostasis (Lim et al. 2017; Russell et al. 2014; Shklover et al. 2015). Concerning the autophagy machinery, the complexity is comparable with human (less genes than yeast but more than *C. elegans, D. melanogaster, C. owczarzaki*, and *M. brevicollis*) (Table 1 – blue column "autophagy" and Supplementary Information SI 10) (Godefroy et al. 2009). For phagocytosis, higher animals have specialized cells, named macrophages. Engulfment of large targets requires phosphoinositide-3- kinase (PI3K) that is activated by Elmo-Dock complexes (Stevenson et al. 2014). This activation leads to disassembly of F-actin and the formation of engulfment vesicles (Schlam et al. 2015). Sponges do not possess this type of specialized cells, but we found 5 *Dock* (versus 10 in human), 1 *Elmo* (versus 3 in human), and 4 *PI3K* (versus 9 in human) transcripts (Table 1 – light grey column "phagocytosis" Supplementary Information SI 9).

Last, we interested in apoptosis, which allows the reduction of cell number in a tightly controlled manner. We found 5 members of the caspase-dependent extrinsic pathway. For the caspase-dependent intrinsic pathways, we found 6 members of the *bcl-2* family, *Bax-inhibitor, Apaf-1 (apoptotic peptidase activating factor* 1*), 4 cytochrome c*, and *omi/HtrA2*. Four *caspase* transcripts bearing the classical signature domains were predicted with two *BIRC* (baculoviral inhibitors of apoptosis repeat containing) inhibitors. Last, we found, for the caspase-independent apoptotic pathway, two *apoptosis-inducing factor (AIF)* transcripts (Table 1 – dark grey column "apoptosis").

The nutrition cycle induces molecular regulation of all the mechanisms involved in homeostasis

As we identified the contributors of the different mechanisms regulating shape homeostasis in the first part of the study, we examined which of these molecular actors were positively or negatively regulated by nutrition cycle. We found that all the mechanisms studied present, although to varying degrees, transcriptional changes in their key actors (Fig. 3).

For stem cell markers, two SoxB1 (a and c) are strongly activated during nutrition with a return to the initial expression rate after 216 h (Fig. 3a). The regulation of the silicate skeleton also seems to be influenced by nutrition, since the silicatein genes α and β are repressed after nutrition (Fig. 3b). With regard to cell cycle regulation, one E2F and four Cdk promoting cell cycle progression are regulated by nutrition: three positively (E2Fa, Cdk4, and Cdk12/13) and two negatively (Cdk7 and Cdk10). Cyclin L and IKBe are rapidly activated, while activation of Wee-1 occurs later (Fig. 3c). In parallel to these observations, we found a marker of phagocytosis, PI3Kgamma that presents a temporary peak of activation at 15 h after the onset of feeding (Fig. 3d). For autophagy, we observe that Vps15 and three ATG genes are negatively regulated with nutrition (ATG2, ATG9, and ATG14). Conversely, the central inhibitor of autophagy, Tor, is activated by nutrition (Fig. 3e). For apoptosis, our

results suggest that the caspase-dependent intrinsic pathway is positively regulated by nutrition (activation of Bcl family member, Apaf-1, Omi/Htra2, and a caspase) concomitantly with inactivation of anti-apoptotic proteins (BIRC5 and BIRC6) (Fig. 3f). At the same time, the transcript encoding AIF, which acts both as an NADH oxidoreductase and as a caspase-independent cell death inducer when it relocates from the mitochondria to the nucleus (Porter and Urbano 2006), is also regulated.

Cell biology analyses support and confirm transcriptomic data

Transcriptomic analysis suggests that the expression of regulators that control the shape during a digestion cycle is modulated at molecular level. Therefore, we conducted an extensive cell biology study to confirm the results obtained by differential transcriptomic analysis.

Confocal microscopy analysis shows the loss of spicules at the top of the filaments 40 h after the capture of a prey and their presence 216 h after catching, i.e., at the end of a digestion cycle (arrow heads in Fig. 4b, c, compared with a). This loss of spicules 40 h after the capture of a prey results in an accumulation of free spicules at the bottom of the beakers (data not shown).

Next, we performed EdU staining to visualize proliferation in the different parts of the sponge during a nutrition cycle. In the peduncle, proliferation spikes strongly between 15 and 40 h after nutrition before returning to resting levels (68% of EdU-positive cells *versus* 11%, 27%, and 9% at 0 h, 15 h, and 216 h, respectively, Fig. 5 and Supplementary Information SI 15). EdU-positive cells were also observed at the base of the filaments after feeding (Supplementary Information SI 14). There was also a significant increase in the number of phagocytes (cells able to ingest particles of various sizes, including other cells) in both the peduncles and apical ovoid bodies of fed sponges (arrowheads, Fig. 6). Last, we studied two mechanisms that can lead to cell death: autophagy and apoptosis. MAPLC3, a marker of autophagy vesicles, was used for immunofluorescent staining of autophagy, while TUNEL staining was performed to highlight apoptosis. The MAPLC3 protein is clearly present in the peduncle cells of unfed animals, whereas it disappears as soon as feeding begins (Fig. 7). In parallel, TUNEL-positive cells were visible as soon as 15 h with an excess at 40 h post-feeding at the end of the filaments (Fig. 8b, c) and, to a lesser extent, in the peduncle (data not shown) with in both cases a return to basal levels 216 h after feeding. These data demonstrate a switch between autophagy and apoptosis upon feeding in sponges.

To test the importance of apoptosis throughout a complete nutrition cycle, we inhibited this mechanism with ZVAD-FMK, a broad-spectrum caspase inhibitor (Fig. 9). Figure 9a–f shows that despite the inhibition of caspases, filaments are able to regress after feeding. Conversely, filament regeneration is not possible when caspase activity is blocked. Contrary to what is observed in the untreated sponge, no apoptotic nucleus is detected in the presence of ZVAD-FMK (Fig. 9g–j). These TUNEL staining results concern the filaments, but the study was also conducted in different parts of the body of the sponge (Supplementary Information SI 12).

Discussion

Throughout its digestion cycle, *L. hypogea* is subject to morphological reorganization under the control of a complex molecular network with respect to cell proliferation, differentiation from stem cells, and programmed cell death.

Complex molecular networks involved in tissue homeostasis are already present at the root of metazoans

Based on a comprehensive phylogenetic study including *Amphimedon queenslandica* (Srivastava et al. 2010), it has been proposed that the evolution of various genes operating in cell cycle, programmed cell death, cell–cell and cell–matrix adhesion, developmental signaling, innate immunity, and cell type specialization has been instrumental in the emergence of metazoan multicellularity. We have studied three of these key mechanisms and a few others in the context of the nutritional cycle.

Stem cell markers. The diversity of *Sox* genes present in *L. hypogea* appears to be comparable to that found in *Drosophila melanogaster* (8 genes), *Caenorhabditis elegans* (5 genes), or *Ciona intestinalis* (6 genes) (Koopman et al. 2004) and probably plays a key role in the cyclic changes in cell identity (Abdelalim et al. 2014) observed during a digestion cycle in *L. hypogea*. *L. hypogea* has the same number of *Sox* genes as calcisponges, but with less diversity and a more abundant repertoire of *SoxB*-related genes, suggesting that the specific expansion of this subfamily occurred in the *L. hypogea* lineage (Fortunato et al. 2012).

Silicate skeleton regulation The spicules of the siliceous sponge provide an exceptional integrative model to follow the distinct hierarchical levels, from genes to molecules, fibrils, fibers, and finally morphology. All the proteins involved in this mechanism are found in *L. hypogea*.

Cell cycle regulation In yeast, one Cdk is associated with several different cyclins, whereas in vertebrates, different Cdk (about 20 in humans) bind to different cyclins (about 30 in humans) to form a complex. We found 12 *Cdk* and 17 *cyclins* in *L. hypogea* with possible duplication of *cyclin B, D, E*, and *T*, which is consistent with the *Amphimedon Cdk/cyclin* gene data (11 predicted *Cdk* and 13 predicted *cyclins*) (Cao et al. 2014 and Supplementary Information SI 10). The absence of *CDKN* strongly suggests that this level of cell cycle regulation appears later in animal evolution.

Autophagy and phagocytosis markers The intake of new nutrients (amino acids, nucleotides, fatty acids, etc.) comes from the catabolism of larger molecules resulting from two main distal mechanisms: autophagy (self-recycling induced by various stresses or cellular conditions, including the absence of food) and phagocytosis (use of ingested food). Our results are consistent with the idea (suggested by our previous work: see movie in Martinand-Mari et al. 2012) that archaeocytes could differentiate into digestive cells in the time needed for the organism to transform prey into usable resources for survival.

Apoptosis *L. hypogea*, which belongs to the sister group of eumetazoans, provides a key phylogenetic model for studying the evolution of cell death at the root of metazoans. We have found that, unlike unicellular organisms, *L. hypogea* possesses members of the extrinsic pathway, even if they are not multiple. The intrinsic pathway is present, and the complexity of the *bcl2* family is significant: 6 putative members compared with 21 in human, 3 in the nematode, and 2 in *Drosophila* (Banjara et al. 2020; Colin 2009). All members of the apoptosome complex are present, and four caspases were predicted, which is comparable to the repertoires of nematode (4 caspases) and fly (7 caspases) in contrast to choanoflagellates that do not have recognizable caspases (Denton et al. 2013; Richter

et al. 2018; Wang and Yang 2016). Among these four caspases, we suspect that Lh-caspase a and b are initiator caspases since they possess a long pro-domain with card domain and DED domain, respectively. Finally, a clear homolog of P53 is present in *L. hypogea*, probably allowing coordinated regulation of apoptosis and cell cycle as observed in metazoans. So, *L. hypogea* potentially possesses all the necessary machinery to achieve all types of apoptosis described in mammals despite its basal phylogenetic position. Interestingly, the extrinsic pathway appears to be less complex than in mammals suggesting that the intrinsic pathway may be the most ancestral. This idea is consistent with a recent work showing that regulators of the mitochondrial machinery, among which some apoptotic factors, are directly involved in the adaptation to aerobic condition (Kaczanowski et al. 2018).

All these results show a clear discrepancy between the reduced number of cell types in *Lycopodina* and the diversity of transcripts involved in cellular functions. This is in line with a recent study carried out on different non-carnivorous sponges (Renard et al. 2018).

The nutrition cycle progression is associated with changes in gene expression levels in correlation with morphological remodeling

We have previously shown that nutrition in *L. hypogea* involves concerted events of programmed cell death and cell proliferation (Martinand-Mari et al. 2012). Here, by obtaining for the first time a *L. hypogea* de novo transcriptome, we have further demonstrated that phenotypic changes in the shape of the organism are associated with a transcriptomic response that mainly fades between 40 h and 9 days after feeding. Indeed, gene expression profiles at 216 h post-feeding and in unfed animals were found to be quite similar (Fig. 2e). This is consistent with the existence of a molecular switch underlying the morphological transformations triggered by prey capture and digestion.

Nutrition cycle is associated with molecular adaptation of all cellular fundamental processes involved in tissue homeostasis

Unfed animals are characterized by high expression level of genes involved in autophagy (Fig. 3e). This is consistent with the survival role of autophagy, which corresponds to a “self-eating” process of cells in the absence of nutrients. This mechanism is important for the recycling of products for immediate or future use. In the same way, the key inhibitor of autophagy, *Tor*, is expressed at its lowest level in unfed animals (Fig. 3e), and MAPLC3 staining demonstrates the presence of active autophagy at this stage (Fig. 7a and Supplementary Information SI 13). This strong involvement of autophagy in unfed animals could explain the ability of *L. hypogea* to live in food-poor environments and to survive several months in the aquarium without any food intake. At the same time, unfed animals with their long stable filaments present a low basal level of proliferation and apoptosis (Figs. 5a and 8a). The absence of nutrients and apoptosis (energy-intensive processes) may be related to the very low level of the phagocytosis marker, *PI3K*, and absence of significant signs of phagocytosis vesicles (Figs. 3d and 6a); indeed, phagocytosis allows the internalization and digestion of *Artemia* vesicles and participates in the clearance and energy recycling of apoptotic bodies. Finally, the specific morphology of unfed animals with their long filaments (Fig. 2a) is associated with a high level of genes involved in silicate skeleton polymerization and stabilization (Fig. 3b). In summary, in the absence of nutrition, a stable shape and transcriptomic signatures corresponding to a morphostatic state are observed.

After contact with Artemia, the morphology of *L. hypogea* changes radically (Fig. 2b, c). The filaments shorten (15 h post-feeding) until they reach the sponge body (40 h post-feeding), and the expression profiles of more than four thousand genes are significantly modified (Fig. 2e). Specifically, the autophagy genes are repressed, while Tor is strongly activated to inhibit autophagy, and this transcriptional regulation is correlated with a disappearance of staining of autophagy vesicles (Figs. 3e and 7b, c). At the same time, food intake rapidly activates the transcription of the phagocytosis marker *PI3K*, and phagocytic vesicles appear to catabolize nutrients (Figs. 3d and 6b, c). Consistent with the phenotypic change in filament size, seven genes of the apoptotic pathway are highly activated: *AIF3*, active in the caspase-independent apoptosis pathway, and six genes involved in the intrinsic/mitochondrial pathway of apoptosis. In the latter, are found *Omi/htrA2* and *Apaf-1*, classically described as activators of caspases, *Caspase-d* and a likely pro-apoptotic member of the *Bcl-2* family **(**Fig. 3f). Finally, the anti-apoptotic gene *survivin* and *BIRC6/Apollon* are rapidly repressed by food intake. In summary, our results suggest that the intrinsic apoptotic and caspase-independent pathways are preferentially involved in the regulation of the shape during a nutrition cycle in *L. hypogea*. The extrinsic pathway is either not involved in this regulation or is involved without any transcriptional regulation. Indeed, protein interactions in large complexes called DISC (death-inducing signaling complex) can lead to non-transcriptional activation of caspases in mammals. However, unlike the mitochondrial pathway, we found few actors of the extrinsic pathway in *L. hypogea*. Mammalian NFκB is involved in both cell cycle induction and apoptosis inhibition. If we compile our cell biology results for apoptosis and cell cycle with negative regulation of *IκB* during feeding, we can assume that NFκB only regulates apoptosis in our model. In parallel, *SoxB1a* and *SoxB1c* are strongly induced by nutrition (Fig. 3a): Sox proteins are transcription factors that play an important role in developmental processes but also in adults. Many of them seem to have conserved functions in eumetazoans (Duffy 2012; Vriz et al. 2014). Sponges have fewer *Sox* genes than eumetazoans, and their roles remain unclear. A study on the calcareous sponge, *Sycon ciliatum*, has shown a model of dynamic expression of the six *Sox* genes in which they can regulate development and cell type determination as in eumetazoans (Fortunato et al. 2012). In these sponges, *SoxB* expression is only embryonic. In the demosponge *Reniera* sp., the three described *Sox* genes (B, C, and F) are differentially expressed during development, but the adult expression is unknown (Larroux et al. 2006). In *L. hypogea*, we show a clear induction of *SoxB* by feeding in adult, and it is particularly tempting to hypothesize a conserved role of the protein in the maintenance of totipotency. In this case, we can postulate that SoxB1 proteins are expressed in archaeocytes (sponge stem cells) that proliferate, transdifferentiate, and migrate after prey capture. It has previously been suggested that in demosponges, archaeocytes ingest, digest, and transmit nutrients to other cells in the sponge (Simpson 1984). Like all stem cells, archaeocytes must also actively proliferate to ensure filament regeneration. This is consistent with the strong increase in proliferation detected by EdU labeling (Fig. 5c), with the increase in *E2Fa*, *cyclin L*, *Cdk4*, and *Cdk12/13* (Fig. 3c) promoting cell cycle progression and the decrease in tumor suppressor *Cdk10* (Yu et al. 2012, p. 10). The activation of *Wee-1* is late, which probably anticipates the reduction in proliferation observed at 216 h. The repression of transcript *Cdk7* is more surprising if its role in *L. hypogea* is comparable to its known role in humans (Sava et al. 2020). Last, it has recently been described in the demosponge *Ephydatia fluviatilis* that cells expressing *SoxB1* served as transport cells responsible for spicules structure formation (Nakayama et al. 2015). In contrast to local skeleton formation in vertebrates, sponge spicules may be assembled far from their place of production, and we propose that the high induction of *SoxB1* is responsible for both the maintenance of

totipotency and spicule transport as evidenced during the dynamic of prey-capture filament morphogenesis. Despite the fact that we see a part of the spicules fallen on the rock when filaments regress, we cannot exclude the fact that a part of the spicules migrates without falling. In this case, the transport could also be directed by *SoxB1*.

From 40 to 216 h after Artemia capture, filaments regenerate to return to their initial state (Fig. 2d), and the gene expression profile tends to come back quite similar to that of unfed individuals (Fig. 2e). The reformation implies the new synthesis and transport of spicules (Fig. 4c, d versus 4 a and b). Expression of genes implicated in autophagy return (more or less depending on the gene) to their initial level (Fig. 3e). Phagocytosis marker *PI3K* decreases to become similar to unfed level (Fig. 3d). Transcripts involved in stem cell maintenance, apoptotic pathway, and proliferation return to their initial level (Fig. 3a, b, c and f). It is important to note that, despite a complete return to the unfed phenotype, the transcriptional status does not return to its initial level for all genes (Figs. 2e and 3).

Counter-intuitively, the transcription of genes of the different studied mechanisms is not sequential but concomitant. Indeed, we do not observe a clear cleavage in time, with an initial induction of apoptosis followed by proliferation and formation of a silicate skeleton. Conversely, we observe a simultaneity of transcriptional regulation suggesting that these processes are tightly interconnected. This observation could also reflect the involvement of many genes in several mechanisms. For example, caspases can regulate differentiation (Bell and Megeney 2017; Solier et al. 2017); cyclins and Cdk can, in complex or independently, regulate apoptosis, cell migration, and differentiation (Hydbring et al. 2016); Bcl-2 allows the interconnection of apoptosis and autophagy, and Atg8 et Atg5 can regulate apoptosis (Thorburn 2008); and Omi/htrA2 could also be involved in cellular homeostasis controlling cell proliferation (Kuninaka et al. 2007). This close interweaving of distinct mechanisms has already been addressed in Porifera since it has been shown in *Suberites domuncula* that survivin plays a conserved regulatory role in the interconnected pathway of cell cycle and apoptosis (Luthringer et al. 2011).

The role of apoptosis in regeneration seems already present at the root of metazoans

It is interesting to note that inhibition of apoptosis in *L. hypogea* gave unexpected results as it does not prevent the shortening of filaments but inhibits their regeneration (Fig. 9). These surprising results suggest that filament shortening could be mainly explained by a massive migration of cells to ingest food. Apoptotic cells are mainly observed at the extremity of the filaments (Supplementary Information SI 12), and we can hypothesize that when filaments regenerate, proliferation and migration act together to reform new filaments. However, these both mechanisms are not sufficient since inhibition of apoptosis after filament regression is sufficient to prevent filament reformation. Studies in models belonging to the eumetazoans have shown that apoptosis can play an important role in regeneration. This apoptosis (regenerative cell death) can act either actively by allowing the release of long or short-distance signals to regenerate or passively by eliminating cells that suppress regeneration (Duffy 2012; Vriz et al. 2014). Our results suggest that this particular role of apoptosis was already present in sponges.

Altogether, our results show that the continuous phenomenon of construction-deconstruction-reconstruction of filaments observed during one digestive cycle is tightly related to a rapid modulation of the molecular networks that control the cellular processes (i.e., proliferation, differentiation, apoptosis) involved in morphological transitions of the prey capture system. We thus witness a succession/coexistence of transcriptional

activation/repression of the molecular networks that control tissue remodeling, one taking over from the other, in perfect agreement with the shape changes observed during a digestion cycle. In addition to the high level of complexity of the molecular actors involved in these networks, our results reveal that the same function or even complex interconnected functions such as the destructive and constructive functions of apoptosis are under the control of the same molecular and cellular networks in all metazoans, regardless of their phylogenetic position. In the sister groups of remaining non-bilateria and bilateria, one thus assists to a regionalization of the nutritive/digestive function: choanocyte chamber with predominant intracellular digestion in sponges, digestive tract with intra and extracellular digestion in ctenophores, “digestive bag” with intra and extracellular digestion in Placozoa, extra and intracellular digestion in a sac-like gastrovascular system in cnidarians, digestive syncytium in most xenacoelomorphs (Gavilán et al. 2019; Steinmetz 2019). In all these groups, food is carried to the digestive system, and the digestive function does not lead to any change in the global morphology of the organism. In carnivorous sponges, the situation is completely different; here, there is no regionalization of the digestive system, and it is the archeocyte/digestive cells, the bacteriocytes, and the symbiotic bacteria that perform the digestive function via intra and extracellular digestion. Cells migrate towards the food, the contact with nutrients being optimized by a complete reorganization of the apical region of the animal. This represents a spectacular example of independent evolution and implies that it is the totality of the cells of the organism (including cells that actively migrate towards the prey from the base of the peduncle; see Martinand Mari et al.) that either directly or indirectly ensures the digestive function. By transcriptomic analysis supported by cell biology experiments, we have been able to identify the main molecular actors that made possible this major evolutionary transition (i.e., the shift from filter feeding provided by a mainly intracellular digestive function to intra and extracellular feeding by prey capture without any regionalization of the digestive system) in the sister group of all other metazoans.
In addition, compared to other models of sponges, *Lycopodina* has the advantage of allowing a study of regeneration on a regular, non-traumatic phenomenon, without an aquifer system to reconstitute (Ereskovsky et al. 2021 2020).

Supplementary information The online version contains supplementary material available at https://doi.org/10.1007/s00441-022-03610-3.

Acknowledgements We thank the Montpellier GenomiX platform (MGX), the Montpellier RIO imaging platform (MRI), and the Montpellier Bioinformatics Biodiversity platform (MBB) (Montpellier, France) for provision of data.

Funding Both the MGX (member of the national infrastructure France- Genomics) and the imaging facility MRI (member of the national infrastructure France-BioImaging) platforms were supported by the French National Research Agency (“Investments for the future,” ANR- 10-INBS-09 and ANR-10-INBS-04, respectively).

Declarations

Ethics approval All applicable international, national, and/or institutional guidelines for the care and use of animals were followed.

Conflict of interest The authors declare no competing interests.

References

Abdelalim EM, Emara MM, Kolatkar PR (2014) The SOX transcription factors as key players in pluripotent stem cells. Stem Cells Dev 23:2687–2699. https://doi.org/10.1089/scd.2014.0297

Banjara S, Suraweera CD, Hinds MG, Kvansakul M (2020) The Bcl-2 family: ancient origins, conserved structures, and divergent mechanisms. Biomolecules 10:128. https://doi.org/10.3390/ biom10010128

Bell RAV, Megeney LA (2017) Evolution of caspase-mediated cell death and differentiation: twins separated at birth. Cell Death Differ. https://doi.org/10.1038/cdd.2017.37

Cao L, Chen F, Yang X, Xu W, Xie J, Yu L (2014) Phylogenetic analysis of CDK and cyclin proteins in premetazoan lineages. BMC Evol Biol 14:10. https://doi.org/10.1186/1471-2148-14-10

Chambers I, Tomlinson SR (2009) The transcriptional foundation of pluripotency. Development 136:2311–2322. https://doi.org/10. 1242/dev.024398

Colin J (2009) Mitochondria, Bcl-2 family proteins and apoptosomes: of worms, flies and men. Front Biosci. https://doi.org/10.2741/3517

Denton S, Aung-Htut MT, Kumar S (2013) Developmentally programmed cell death in Drosophila. Biochim Biophys Acta (BBA) Mol Cell Res 1833:3499–3506. https://doi.org/10.1016/j.bbamcr. 2013.06.014

Duffy DJ (2012) Instructive reconstruction: a new role for apoptosis in pattern formation: Instructive apoptotic patterning establishes de novo tissue generation via the apoptosis linked production of morphogenic signals. BioEssays 34:561–564. https://doi.org/ 10.1002/bies.201200018

Dunn CW, Leys SP, Haddock SHD (2015) The hidden biology of sponges and ctenophores. Trends Ecol Evol 30:282–291. https:// doi.org/10.1016/j.tree.2015.03.003

Ereskovsky A (2018) Stem cells cell in sponges (Porifera): an update. 2nd General Meeting and Working Group Meetings of the COST Action 16203: stem cells of marine/aquatic invertebrates: from basic research to innovative Applications (Maristem), November 28–30, 2018, Marine Biology Station. Banyuls-sur-Mer, France

Ereskovsky A, Borisenko IE, Bolshakov FV, Lavrov AI (2021) Whole-body regeneration in sponges: diversity, fine mechanisms, and future prospects. Genes (basel) 12:506. https://doi.org/10.3390/ genes12040506

Ereskovsky AV, Tokina DB, Saidov DM, Baghdiguian S, Le Goff E, Lavrov AI (2020) Transdifferentiation and mesenchymal-to-epithelial transition during regeneration in Demospongiae (Porifera). J Exp Zool (Mol Dev Evol) 334:37–58. https://doi.org/10.1002/jez.b.22919

Fortunato S, Adamski M, Bergum B, Guder C, Jordal S, Leininger S, Zwafink C, Rapp HT, Adamska M (2012) Genome-wide analysis of the sox family in the calcareous sponge Sycon ciliatum: multiple genes with unique expression patterns. Evo Devo 3:14. https://doi.org/10.1186/2041-9139-3-14

Funayama N (2013) The stem cell system in demosponges: suggested involvement of two types of cells: archeocytes (active stem cells) and choanocytes (food-entrapping flagellated cells). Dev Genes Evol 223:23–38. https://doi.org/10.1007/s00427-012-0417-5

Funayama N, Nakatsukasa M, Mohri K, Masuda Y, Agata K (2010) Piwi expression in archeocytes and choanocytes in demosponges: insights into the stem cell system in demosponges. Evol Dev 12:275–287. https://doi.org/10.1111/j.1525-142X.2010.00413.x

Gavilán B, Sprecher SG, Hartenstein V, Martinez P (2019) The digestive system of xenacoelomorphs. Cell Tissue Res 377:369–382. https://doi.org/10.1007/s00441-019-03038-2

Godefroy N, Hoa C, Tsokanos F, Le Goff E, Douzery EJP, Baghdiguian S, Martinand-Mari C (2009) Identification of autophagy genes in Ciona intestinalis: a new experimental model to study autophagy mechanism. Autophagy 5:805–815

Godefroy N, Le Goff E, Martinand-Mari C, Belkhir K, Vacelet J, Baghdiguian S (2019) Sponge digestive system diversity and evolution: filter feeding to carnivory. Cell Tissue Res. https:// doi.org/10.1007/s00441-019-03032-8

Hydbring P, Malumbres M, Sicinski P (2016) Non-canonical functions of cell cycle cyclins and cyclin-dependent kinases. Nat Rev Mol Cell Biol 17:280–292. https://doi.org/10.1038/nrm.2016.27

Kaczanowski S, Klim J, Zielenkiewicz U (2018) An apoptotic and endo-symbiotic explanation of the Warburg and the inverse Warburg hypotheses. IJMS 19:3100. https://doi.org/10.3390/ijms19103100

Kashyap V, Rezende NC, Scotland KB, Shaffer SM, Persson JL, Gudas LJ, Mongan NP (2009) Regulation of stem cell pluripotency and differentiation involves a mutual regulatory circuit of the NANOG, OCT4, and SOX2 pluripotency transcription factors with polycomb repressive complexes and stem cell microRNAs. Stem Cells Dev 18:1093–1108. https://doi.org/10.1089/scd.2009.0113

Koopman P, Schepers G, Brenner S, Venkatesh B (2004) Origin and diversity of the Sox transcription factor gene family: genome-wide analysis in Fugu rubripes. Gene 328:177–186. https://doi.org/10. 1016/j.gene.2003.12.008

Kübler B, Barthel D (1999) A carnivorous sponge, Chondrocladia gigantea (Porifera: Demospongiae: *Cladorhizidae*), the giant deep-sea clubsponge from the Norwegian Trench. Mem Queensl Mus 44:289–297

Kuninaka S, Iida S-I, Hara T, Nomura M, Naoe H, Morisaki T, Nitta M, Arima Y, Mimori T, Yonehara S, Saya H (2007) Serine protease Omi/HtrA2 targets WARTS kinase to control cell proliferation. Oncogene 26:2395–2406. https://doi.org/10.1038/sj.onc.1210042

Larroux C, Fahey B, Liubicich D, Hinman VF, Gauthier M, Gongora M, Green K, Wörheide G, Leys SP, Degnan BM (2006) Developmental expression of transcription factor genes in a demosponge: insights into the origin of metazoan multicellularity. Evol Dev 8:150–173. https://doi.org/10.1111/j.1525-142X.2006.00086.x

Le Goff E, Martinand-Mari C, Martin M, Feuillard J, Boublik Y, Godefroy N, Mangeat P, Baghdiguian S, Cavalli G (2015) Enhancer of zeste acts as a major developmental regulator of Ciona intestinalis embryogenesis. Biol Open bio.010835. https://doi.org/10.1242/ bio.010835

Lim JJ, Grinstein S, Roth Z (2017) Diversity and versatility of phagocytosis: roles in innate immunity, tissue remodeling, and homeostasis. Front Cell Infect Microbiol 7:191. https://doi.org/10.3389/fcimb. 2017.00191

Lim S, Kaldis P (2013) Cdks, cyclins and CKIs: roles beyond cell cycle regulation. Development 140:3079–3093. https://doi.org/ 10.1242/dev.091744

Luthringer B, Isbert S, Müller WEG, Zilberberg C, Thakur NL, Wörheide G, Stauber RH, Kelve M, Wiens M (2011) Poriferan survivin exhibits a conserved regulatory role in the interconnected pathways of cell cycle and apoptosis. Cell Death Differ 18:201–213. https://doi.org/ 10.1038/cdd.2010.87

Martinand-Mari C, Vacelet J, Nickel M, Wörheide G, Mangeat P, Baghdiguian S (2012) Cell death and renewal during prey capture and digestion in the carnivorous sponge Asbestopluma hypogea (Porifera: Poecilosclerida). J Exp Biol 215:3937–3943. https://doi.org/10.1242/jeb.072371

Müller WEG, Link T, Schröder HC, Korzhev M, Neufurth M, Brandt D, Wang X (2014) Dissection of the structure-forming activity from the structure-guiding activity of silicatein: a biomimetic molecular approach to print optical fibers. J Mater Chem B 2:5368. https://doi.org/10.1039/C4TB00801D

Nakayama S, Arima K, Kawai K, Mohri K, Inui C, Sugano W, Koba H, Tamada K, Nakata YJ, Kishimoto K, Arai-Shindo M, Kojima C, Matsumoto T, Fujimori T, Agata K, Funayama N (2015) Dynamic transport and cementation of skeletal elements build up the pole-and-beam structured skeleton of sponges. Curr Biol 25:2549–2554. https://doi.org/10.1016/j.cub.2015.08.023

Okamoto K, Nakatsukasa M, Alié A, Masuda Y, Agata K, Funayama N (2012) The active stem cell specific expression of sponge Musashi homolog EflMsiA suggests its involvement in maintaining the stem cell state. Mech Dev 129:24–37. https://doi.org/10.1016/j. mod.2012.03.001

Porter AG, Urbano AGL (2006) Does apoptosis-inducing factor (AIF) have both life and death functions in cells? BioEssays 28:834– 843. https://doi.org/10.1002/bies.20444

Redmond AK, McLysaght A (2021) Evidence for sponges as sister to all other animals from partitioned phylogenomics with mixture models and recoding. Nat Commun 12:1783. https://doi.org/10. 1038/s41467-021-22074-7

Renard E, Leys SP, Wörheide G, Borchiellini C (2018) Understanding animal evolution: the added value of sponge transcriptomics and genomics: the disconnect between gene content and body plan evolution. BioEssays 40:1700237. https://doi.org/10.1002/bies. 201700237

Richter DJ, Fozouni P, Eisen MB, King N (2018) Gene family innovation, conservation and loss on the animal stem lineage. eLife 7:e34226. https://doi.org/10.7554/eLife.34226

Rinkevich B, Ballarin L, Martinez P, Somorjai I, Ben-Hamo O, Borisenko I, Berezikov E, Ereskovsky A, Gazave E, Khnykin D, Manni L, Petukhova O, Rosner A, Röttinger E, Spagnuolo A, Sugni M, Tiozzo S, Hobmayer B (2022) A pan-

metazoan concept for adult stem cells: the wobbling Penrose landscape. Biol Rev Camb Philos Soc 97:299–325. https://doi.org/10.1111/brv.12801

Russell RC, Yuan H-X, Guan K-L (2014) Autophagy regulation by nutrient signaling. Cell Res 24:42–57. https://doi.org/10.1038/cr. 2013.166

Sava GP, Fan H, Coombes RC, Buluwela L, Ali S (2020) CDK7 inhibitors as anticancer drugs. Cancer Metastasis Rev. https://doi.org/ 10.1007/s10555-020-09885-8

Schlam D, Bagshaw RD, Freeman SA, Collins RF, Pawson T, Fairn GD, Grinstein S (2015) Phosphoinositide 3-kinase enables phagocytosis of large particles by terminating actin assembly through Rac/Cdc42 GTPase-activating proteins. Nat Commun 6:8623. https://doi.org/10.1038/ncomms9623

Shklover J, Levy-Adam F, Kurant E (2015) Apoptotic cell clearance in development current topics in developmental biology. Elsevier, pp 297–334. https://doi.org/10.1016/bs.ctdb.2015.07.024

Simion P, Philippe H, Baurain D, Jager M, Richter DJ, Di Franco A, Roure B, Satoh N, Quéinnec É, Ereskovsky A, Lapébie P, Corre E, Delsuc F, King N, Wörheide G, Manuel M (2017) A large and consistent phylogenomic dataset supports sponges as the sister group to all other animals. Curr Biol. https://doi.org/10.1016/j. cub.2017.02.031

Simpson (1984) The cell biology of sponges. Springer-Verlag, New York. https://doi.org/10.1007/978-1-4612-5214-6

Solier S, Fontenay M, Vainchenker W, Droin N, Solary E (2017) Non-apoptotic functions of caspases in myeloid cell differentiation. Cell Death Differ. https://doi.org/10.1038/cdd.2017.19

Srivastava M, Simakov O, Chapman J, Fahey B, Gauthier MEA, Mitros T, Richards GS, Conaco C, Dacre M, Hellsten U, Larroux C, Putnam NH, Stanke M, Adamska M, Darling A, Degnan SM, Oakley TH, Plachetzki DC, Zhai Y, Adamski M, Calcino A, Cummins SF, Goodstein DM, Harris C, Jackson DJ, Leys SP, Shu S, Woodcroft BJ, Vervoort M, Kosik KS, Manning G, Degnan BM, Rokhsar DS (2010) The Amphimedon queenslandica genome and the evolution of animal complexity. Nature 466:720–726. https://doi.org/10.1038/nature09201

Steinmetz PRH (2019) A non-bilaterian perspective on the development and evolution of animal digestive systems. Cell Tissue Res 377:321–339. https://doi.org/10.1007/s00441-019-03075-x

Stevenson C, de la Rosa G, Anderson CS, Murphy PS, Capece T, Kim M, Elliott MR (2014) Essential role of Elmo1 in Dock2-dependent lymphocyte migration. J Immunol 192:6062–6070. https://doi.org/ 10.4049/jimmunol.1303348

Thorburn A (2008) Apoptosis and autophagy: regulatory connections between two supposedly different processes. Apoptosis 13:1–9. https://doi.org/10.1007/s10495-007-0154-9

Vacelet J (1996) Deep-sea sponge in a Mediterranean cave. In: Uiblein F (ed) deap-sea and extreme shallow water habitats: affinities and adaptations. J Ott and M Stachowitsch Austrian Academy of Sciences, Vienna, pp 299–312

Vacelet J, Boury-Esnault N (1996) A new species of carnivorous sponge (Demospongiae: *Cladorhizidae*) from a Mediterranean cave. Med K Belg Inst Nat Wet 66(Suppl.):109–115

Vacelet J, Boury-Esnault N (1995) Carnivorous sponges. Nature 333–335

Vacelet J, Duport E (2004) Prey capture and digestion in the carnivorous sponge Asbestopluma hypogea (Porifera: Demospongiae). Zoomorphology 123:179–190. https://doi.org/10.1007/ s00435-004-0100-0

Vriz S, Reiter S, Galliot B (2014) Cell death current topics in developmental biology. Elsevier, pp 121–151. https://doi.org/10.1016/ B978-0-12-391498-9.00002-4

Wang X, Schloßmacher U, Wiens M, Batel R, Schröder HC, Müller WEG (2012) Silicateins, silicatein interactors and cellular interplay in sponge skeletogenesis: formation of glass fiber-like spicules: silicateins/silicatein interactors in spiculogenesis. FEBS J 279:1721–1736. https://doi.org/10.1111/j.1742-4658.2012. 08533.x

Wang X, Yang C (2016) Programmed cell death and clearance of cell corpses in Caenorhabditis elegans. Cell Mol Life Sci 73:2221– 2236. https://doi.org/10.1007/s00018-016-2196-z

Yu J-H, Zhong X-Y, Zhang W-G, Wang Z-D, Dong Q, Tai S, Li H, Cui Y-F (2012) CDK10 functions as a tumor suppressor gene and regulates survivability of biliary tract cancer cells. Oncol Rep 27:1266–1276. https://doi.org/10.3892/or.2011.1617

Table 1 Proteins of the different mechanisms studied (named in different colors depending on the mechanism) found in *Lycopodina hypogea de novo* transcriptome. Red, identity and stem cell markers; orange, spicule skeleton; purple, cell cycle control; light grey phagocytosis; blue, autophagy; and dark grey, apoptosis. Transcripts that were not found are listed in white on a grey background

Cellular identity and stem cell markers		Cell cycle control		Phagocytosis	Autophagy		Apoptosis	
Nanog	Stem cell	Lh-E2Fa		Lh-Dock-1	Lh-ATG 1		Lh-TNFRSF	Extrinsic pathway
Oct-4		Lh-E2Fb		Lh-Dock-1/2	Lh-ATG 2		Lh-FAF1	
Lh-Sox B1a		Lh-E2Fc		Lh-Dock-3*	Lh-ATG 3		Lh-FAF2	
Lh-Sox B1b		Lh-E2Fd		Lh-Dock-7	Lh-ATG 4ab		Lh-FAIMa	
Lh-Sox B1c		Lh-DP		Lh-Dock-9	Lh-ATG 4cd		Lh-FAIMb	
Lh-Sox B2		Lh-Rb		Lh-ELMO	Lh-ATG 5		Lh-Fadd	
Lh-Sox C		Lh-cdk1	cdk family	Lh-PI3K alpha	Lh-ATG 6/beclin		Lh-Bcl family a	Intrinsec pathway
Lh-Sox F		Lh-cdk2		Lh-PI3K beta	Lh-ATG 7		Lh-Bcl family b	
Lh-musashi 1		Lh-cdk4		Lh-beta/delta a	Lh-GABARAPa	ATG 8	Lh-Bcl family c	
Lh-musashi 2		Lh-cdk5		Lh-PI3K beta/delta b	Lh-GABARAPb		Lh-Bcl family d	
Lh-PIWI 1		Lh-cdk7		Lh-PI3K gamma	Lh-GABARAPc		Lh-Bcl family e	
Lh-PIWI 2		Lh-cdk9			Lh-GABARAPd		Lh-Bcl family f	
Lh-RTKvs	Archaeocytes	Lh-cdk-10			Lh-GABARAPe		Lh-Bcl family g	
Lh-Iroquois	Pinacocytes	Lh-cdk11B			Lh-MAP1LC3a		BH3-only	
Lh-Myotrophin	Myocytes	Lh-cdk12 /13			Lh-MAP1LC3b		Lh-bax inhibitor 1	
Lh-Silicatein alpha	Sclerocytes	Lh-cdk14			Lh-MAP1LC3c		Lh-apaf-1	
Lh-Silicatein beta		Lh-cdk18			Lh-MAP1LC3d		Lh-Cyt c-a	
Lh-Silintaphin		Lh-cdk20			Lh-MAP1LC3e		Lh-Cyt c-b	
Lh-Silicase		Lh-Cyclin-A2	Cyclin family		Lh-MAP1LC3f		Lh-Cyt c-c	
Lh-Galectin		Lh-Cyclin-B			Lh-ATG 9		Lh-Cyt c-d	
		Lh-Cyclin-B3a			Lh-ATG 10		Lh-Omi/HtrA2	
		Lh-Cyclin-B3b			Lh-RB1CC1/FIP200		Smac/Diablo	
		Lh-Cyclin-C			Lh-ATG 12		Lh-caspase a	Caspases and inhibitors
		Lh-Cyclin-Da			Lh-ATG 13		Lh-caspase b	
		Lh-Cyclin-Db			Lh-ATG14		Lh-caspase c	
		Lh-Cyclin-E1a			ATG 15		Lh-caspase d	
		Lh-Cyclin-E1b			Lh-ATG 16		Lh-BIRC5/survivin	
		Lh-Cyclin-F			ATG 17		Lh-BIRC6	
		Lh-Cyclin-H			Lh-ATG 18		Lh-CAD	CAD / ICAD
		Lh-Cyclin-I			ATG 19		ICAD/DFF45	
		Lh-Cyclin-K			ATG 20		Lh-AIF1	Capspase-independ.
		Lh-Cyclin-L			ATG 21		Lh-AIF3	
		Lh-Cyclin-Ta			ATG 23		EndoG	
		Lh-Cyclin-Tb			Lh-ATG 24			
		Lh-Cyclin-Y			ATG 26			
		p16/INK4a	CKI		ATG 27			
		p16/INK4b			ATG 29			
		p16/INK4c			Lh-ATG101			
		p16/INK4d			Lh-Vps15			
		p21/CIP1			Lh-Vps34			
		p27/KIP1			Lh-UVRAG			
		p57/KIP2			Lh-Bif-1			
		Lh-Wee-1			Lh-Dram-a			
		Lh-p53			Lh-Dram-b			
		Lh-myc			Lh-Tor			
		Lh-NF-KB			UTH1			
		Lh-IKBE						

Figures

Fig.1 Overview of the different parts of the sponge *Lycopodina hypogea*. Scale bar = 2 mm

Fig.2 Morpho-nutritional cycle of *Lycopodina hypogea*. Fluorescence stereomicroscope images with DAPI staining unfed animal (**a**), and 15 h (**b**), 40 h post-nutrition (**c**), and 216 h (**d**) post-nutrition stages. Arrowhead: nucleus of Artemia nauplii (prey). Orange dotted line: outline of nauplius. Inset: Magnification of an Artemia nauplii. Scale bar=0.5 mm. Gene expression profile of regulated genes after nutrition (**e**). Four conditions are studied 0 h, 15 h, 40 h, and 216 h after feeding for two individuals in each condition (A and B)

Fig. 3 Gene expression diagrams of genes regulated positively or negatively (> fourfold). The color code is the same as in Table 1: red, Identity and stem cell markers; orange, spicule skeleton; purple, cell cycle control; light grey, phagocytosis; blue, autophagy and dark grey, apoptosis

Fig. 4 Dynamics of spicule loss and reformation during a digestion cycle. Confocal microscopy images with DIC on siliceous spicules at top of the filament during a morpho-nutritional cycle: unfed (**a**), 15 h post-nutrition (**b**), post-nutrition (**c**), 216 h post-nutrition (**d**). Arrowhead: silicate filaments. Scale bar = 24 µm

Fig.5 Proliferation during a nutrition cycle. DIC confocal microscopy images showing EdU (cell proliferation in red) and DAPI (in blue) staining in *L. hypogea* peduncles during a nutrition cycle: unfed (**a**), 15 h post-nutrition (**b**), 40 h post-nutrition (**c**), 216 h post- nutrition (**d**). White dotted lines delimit peduncle area. For each stage, the percentage of EdU-positive nucleus is reported as well as the total number of nuclei (*n*: DAPI-positive nuclei). *n* value is representative of 3 independent experiences. Arrowhead: EdU-positive nucleus. Scale bar=20 µm. Mean percentage of positive EdU nuclei among sponges that were unfed, 15, 40, or 216 h post-nutrition (**e**). Error bars indicate the standard error of the mean. <ns> indicates a non-significant difference with *p* value>0.01 (prop.test, R soft- ware); <**> indicates a significant difference with *p* value<0.001 (prop.test, R software); <***> indicates a significant difference with *p* value < 0.0001 (prop.test, R software). See Supplementary Information SI 15 for the complete statistical results

Fig. 6 Phagocytosis during a nutrition cycle. Microscopy images with Toluidine Blue staining, allowing to visualize phagocytosis vesicles (arrows), during a *L. hypogea* nutrition cycle: unfed sponge peduncle (**a**), unfed sponge apical ovoid body (**b**), fed sponge peduncle (**c**), and fed sponge apical ovoid body (**d**). Orange dotted line: phagocyte (spherulous cell). Yellow dotted line: archaeocyte. Scale bar: **a** = 30 µm, **b** and **c**=20 µm, **d**=10 µm

Fig.7 Autophagy during a nutrition cycle. Confocal microscopy images with MAPLC3 (autophagy, in green) and DAPI (in blue) staining in *L. hypogea* peduncles during a morpho-nutritional cycle: unfed (**a**), 15 h post-nutrition (**b**), 40 h post-nutrition (**c**), 216 h post-nutrition (**d**). Dotted lines delimit the peduncle area. Arrowhead: autophagy vesicle. Scale bar = 12 µm

Fig.8 Apoptosis during a nutrition cycle. Confocal microscopy images with TUNEL (apoptosis, in red) and DAPI (in blue) staining in *L. hypogea* filaments during a nutrition cycle: unfed (**a**), 15 h post-nutrition (**b**), 40 h post-nutrition (**c**), 216 h post-nutrition (**d**). White dotted lines delimit filament area. For each stage, the percentage of TUNEL-positive nuclei is reported as well as the total number of nuclei (*n*: DAPI-positive nuclei). *n* value is representative of 3 independent experiments. Arrowhead: TUNEL-positive nucleus. Scale bar=12 µm. Mean percentage of positive TUNEL nuclei among sponges that were unfed, 15, 40, or 216 h post-nutrition (**e**). Error bars indicate the standard error of the mean. <ns> indicates an insignificant difference with *p* value > 0.01 (prop.test, R soft- ware); <**> indicates a significant difference with *p* value < 0.001 (prop.test, R software); <***> indicates a significant difference with *p* value < 0.0001 (prop.test, R software). See Supplementary Information SI 15 for the complete statistical results

Fig.9 Apoptosis inhibition with ZVAD-FMK during a nutrition cycle. Stereomicroscope images at different stages of a morpho-nutritional cycle of *Lycopodina hypogea* (**a–f**): control fed 0 h post-nutrition (**a**), control fed 15 h post-nutrition (**b**), control fed 7 days post-nutrition (**c**), ZVAD-FMK fed 0 h post-nutrition (**d**), ZVAD-FMK fed 15 h post-nutrition (**e**), ZVAD-FMK fed 7 days post-nutrition (**f**). Scale bar **a–f**=2 mm. Confocal microscopy images with TUNEL (apoptosis, in green) and DAPI (in blue) staining in *L. hypogea* filaments during filaments regression and regeneration with or without ZVAD-FMK: control fed 15 h post-nutrition (**g**), ZVAD-FMK fed 15 h post-nutrition (**h**), control fed 7 days post-nutrition (**i**), ZVAD- FMK fed 7 days post-nutrition (**j**). White dotted lines delimit filament area (**g–i**) and apical ovoid body area in **j** because there is no filament regeneration with ZVAD-FMK. For each stage, the percentage of TUNEL-positive nuclei is reported as well as the total number of nuclei (*n*: DAPI-positive nuclei). *n* value is representative of 3 independent experiments. Scale bar **g–j**=30 µm. The active sites of the caspases recognized by the ZVAD-FMK are present in *L. hypogea* caspases, and their sequences are underlined in bold in Supplementary Information SI 6. Mean percentage of positive TUNEL nuclei among sponges during filament regression or regeneration, in presence of ZVAD-FMK or not (**e**). Error bars indicate the standard error of the mean. <*> indicates a significant difference with *p* value<0.01 (prop.test, R software); <***> indicates a significant difference with *p* value<0.0001 (prop.test, R software). See Supplementary Information SI 15 for the complete statistical results

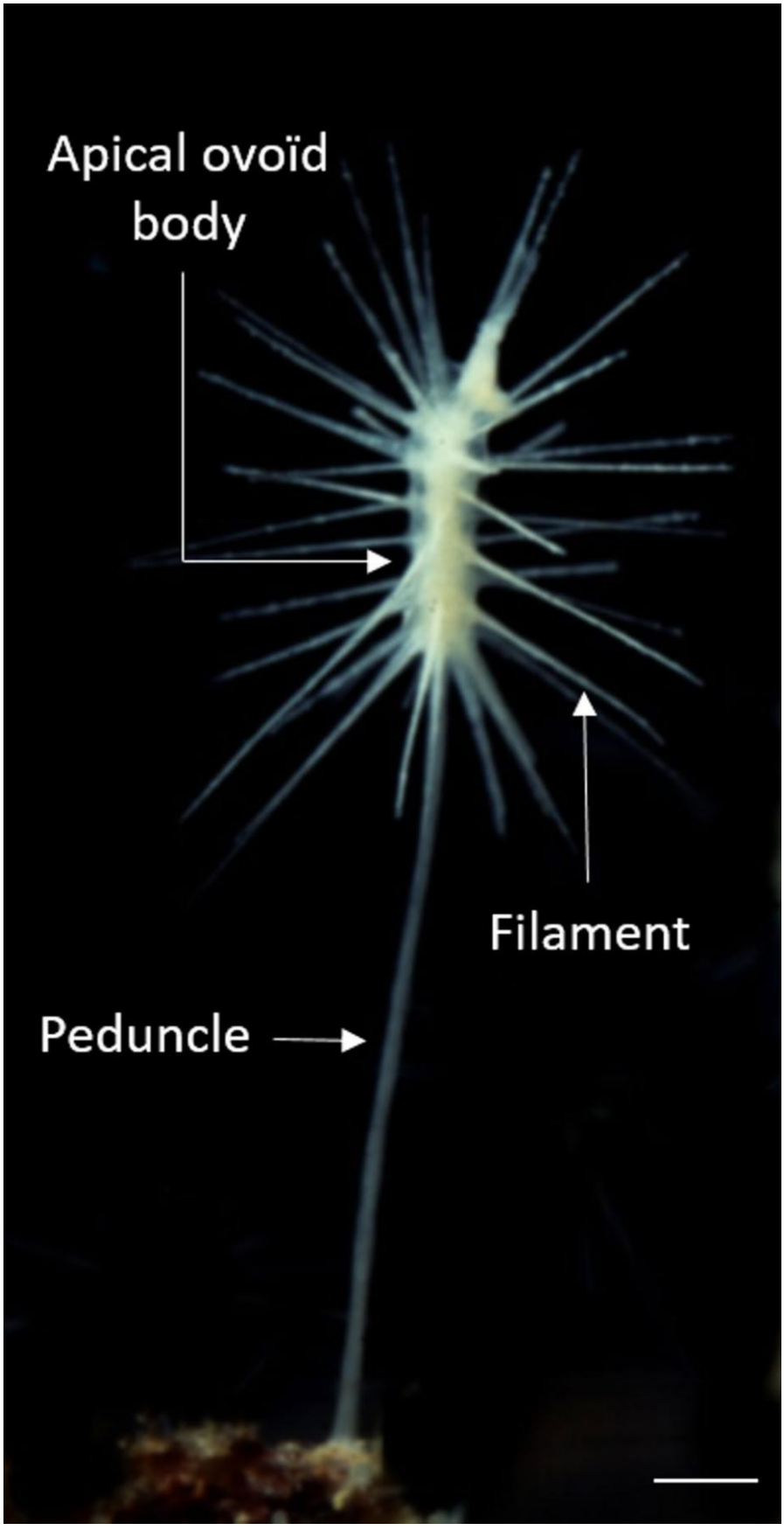

Figure 1

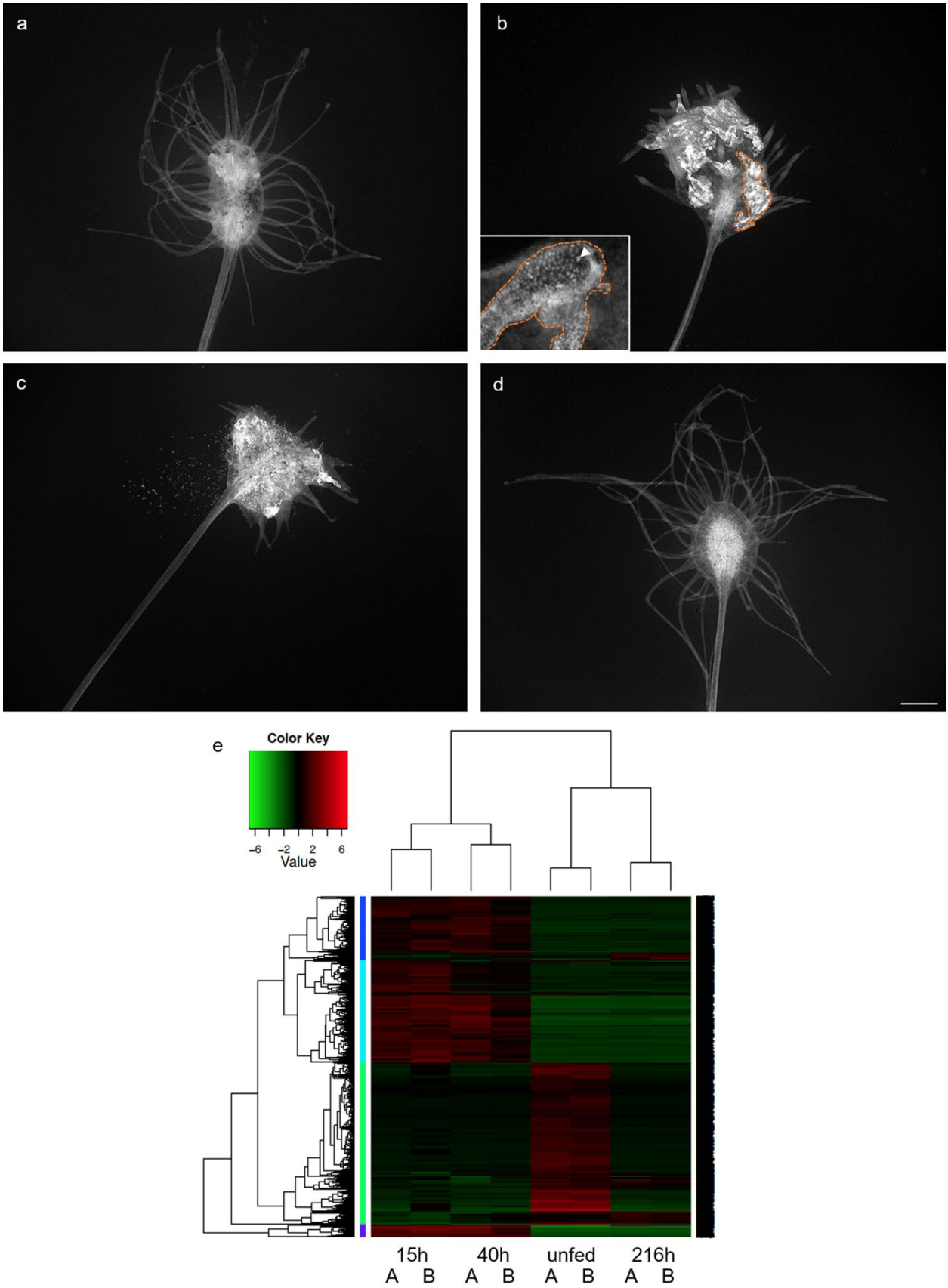

Figure 2

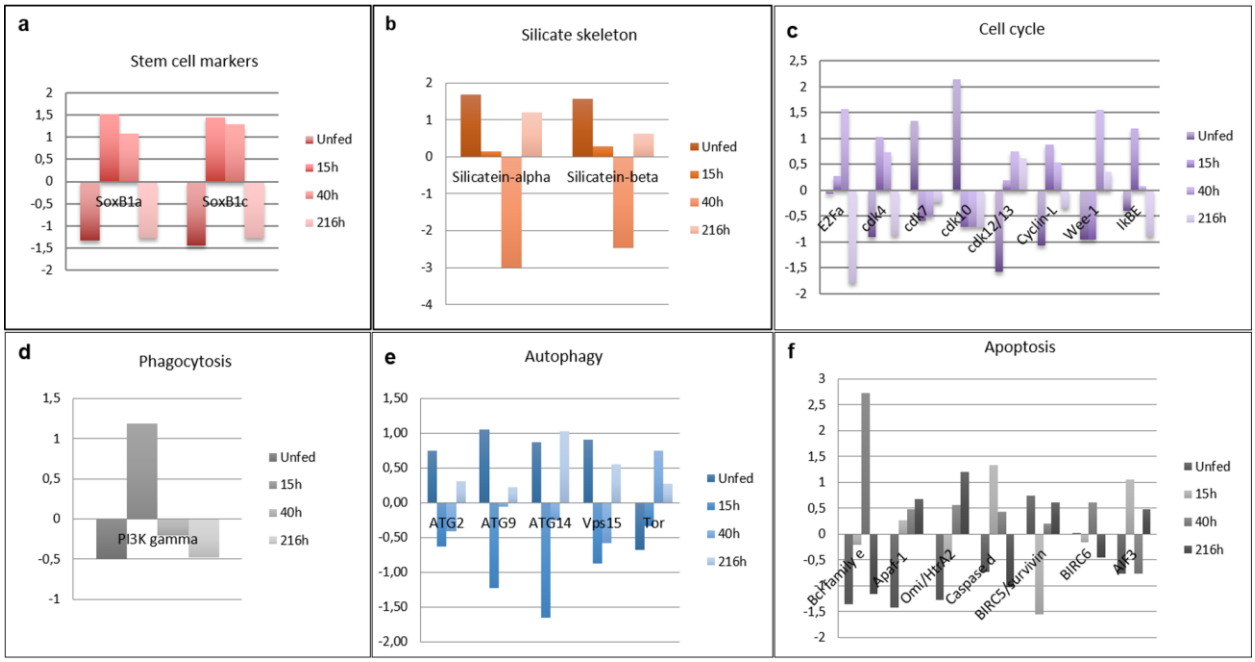
a
Stem cell markers
SoxB1a
SoxB1c
Unfed
15h
40h
216h
b
Silicate skeleton
Silicatein-alpha
Silicatein-beta
Unfed
15h
40h
216h
c
Cell cycle
E2Fa
cdk4
cdk7
cdk10
cdk12/13
Cyclin-L
Wee-1
IkBE
Unfed
15h
40h
216h
d
Phagocytosis
PI3K gamma
Unfed
15h
40h
216h
e
Autophagy
ATG2
ATG9
ATG14
Vps15
Tor
Unfed
15h
40h
216h
f
Apoptosis
Bcl-2 family e
Apaf-1
Omi/Htra2
Caspase-d
BIRC5/survivin
BIRC6
AIF3
Unfed
15h
40h
216h

Figure 3

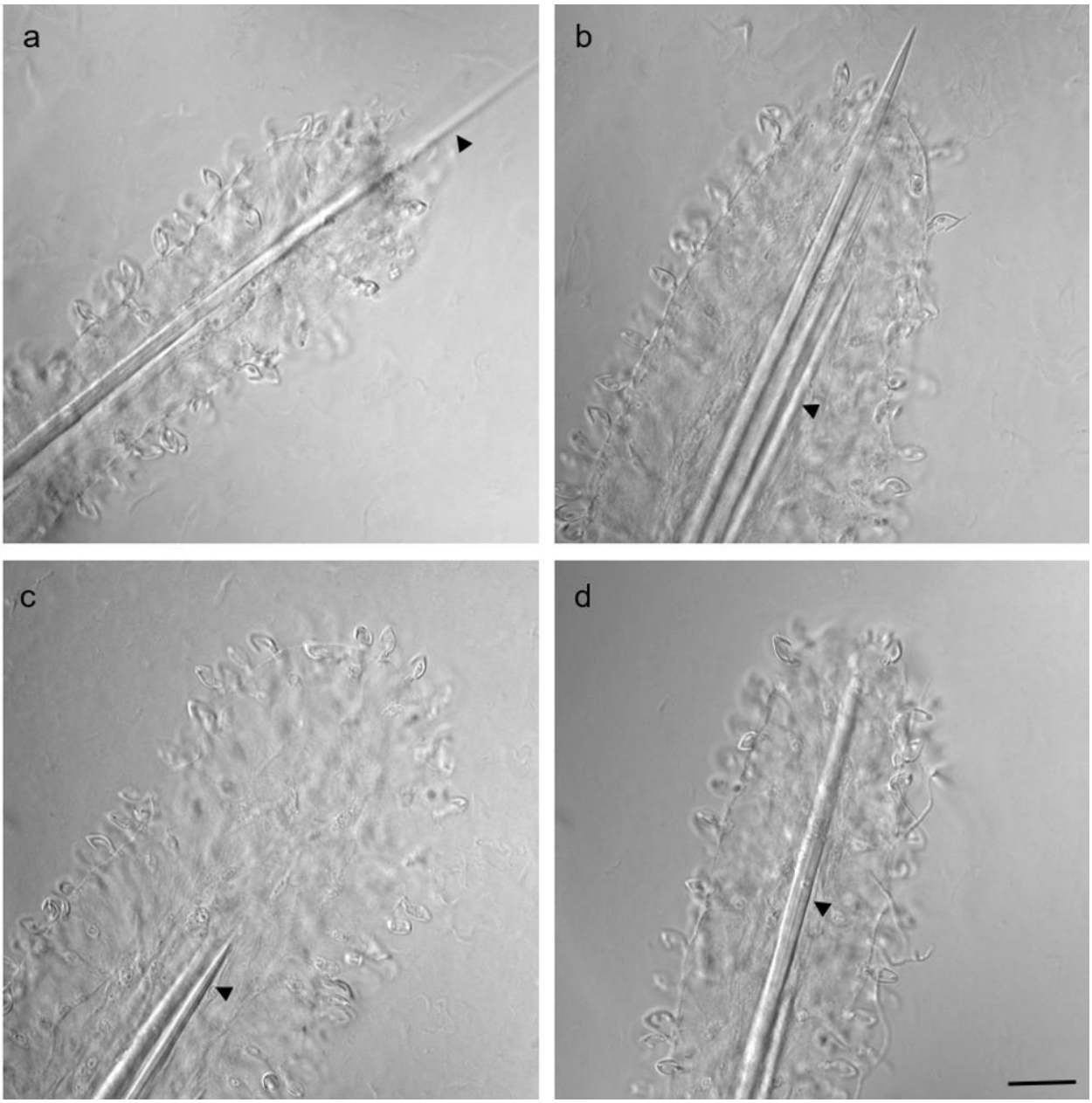

Figure 4

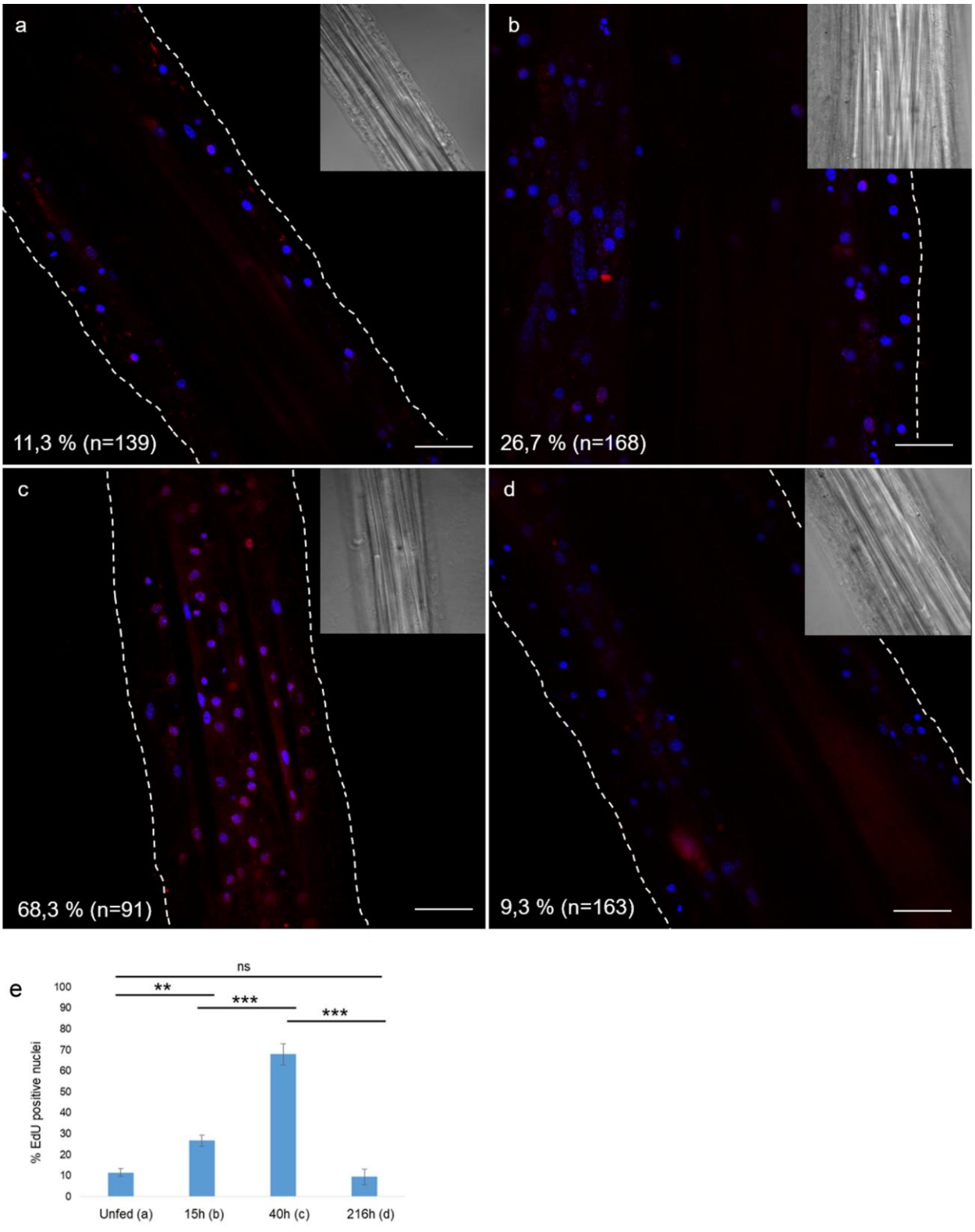
a
11,3 % (n=139)
b
26,7 % (n=168)
c
68,3 % (n=91)
d
9,3 % (n=163)
e
ns
**
***
***
% EdU positive nuclei
100
90
80
70
60
50
40
30
20
10
0
Unfed (a)
15h (b)
40h (c)
216h (d)

Figure 5

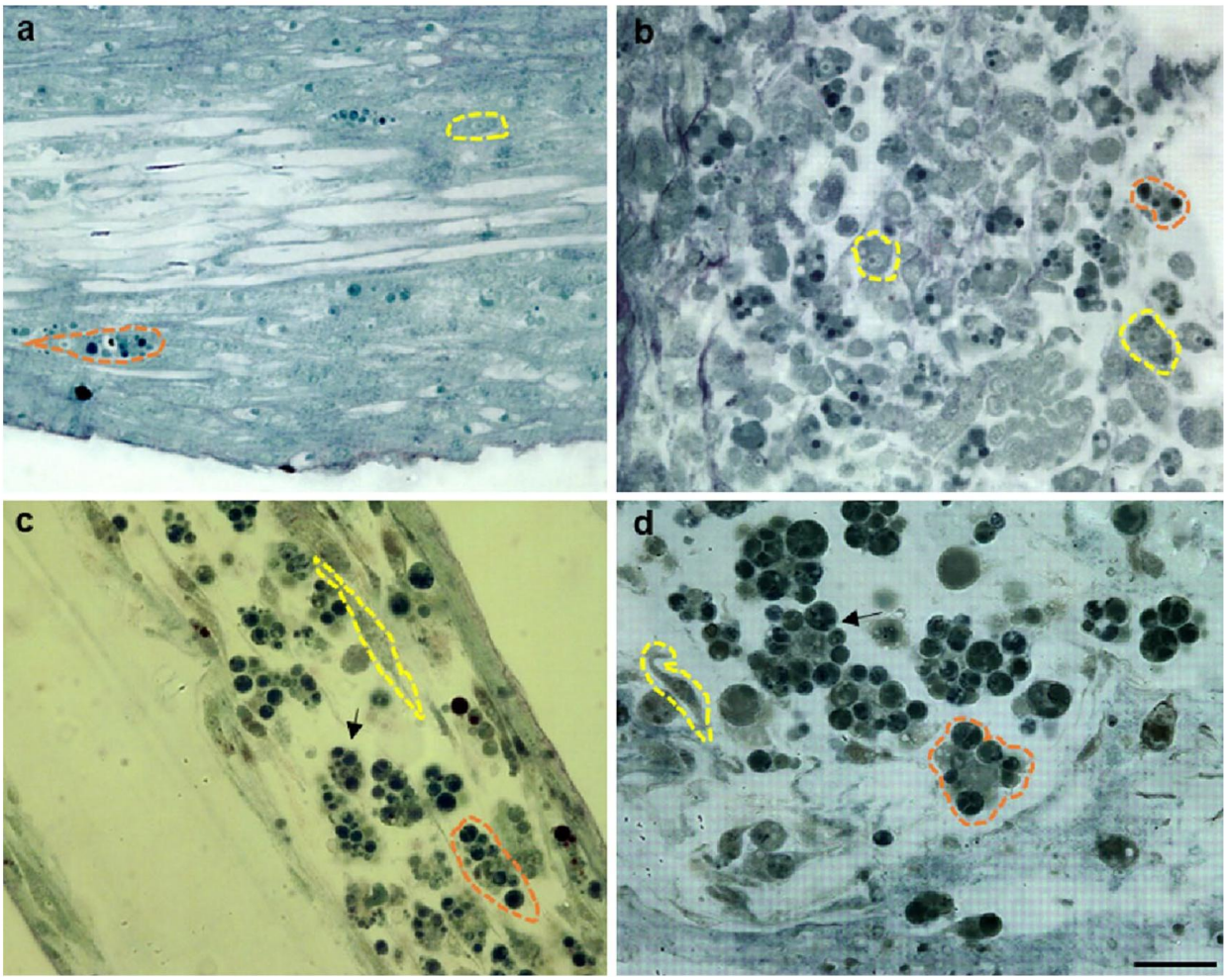

Figure 6

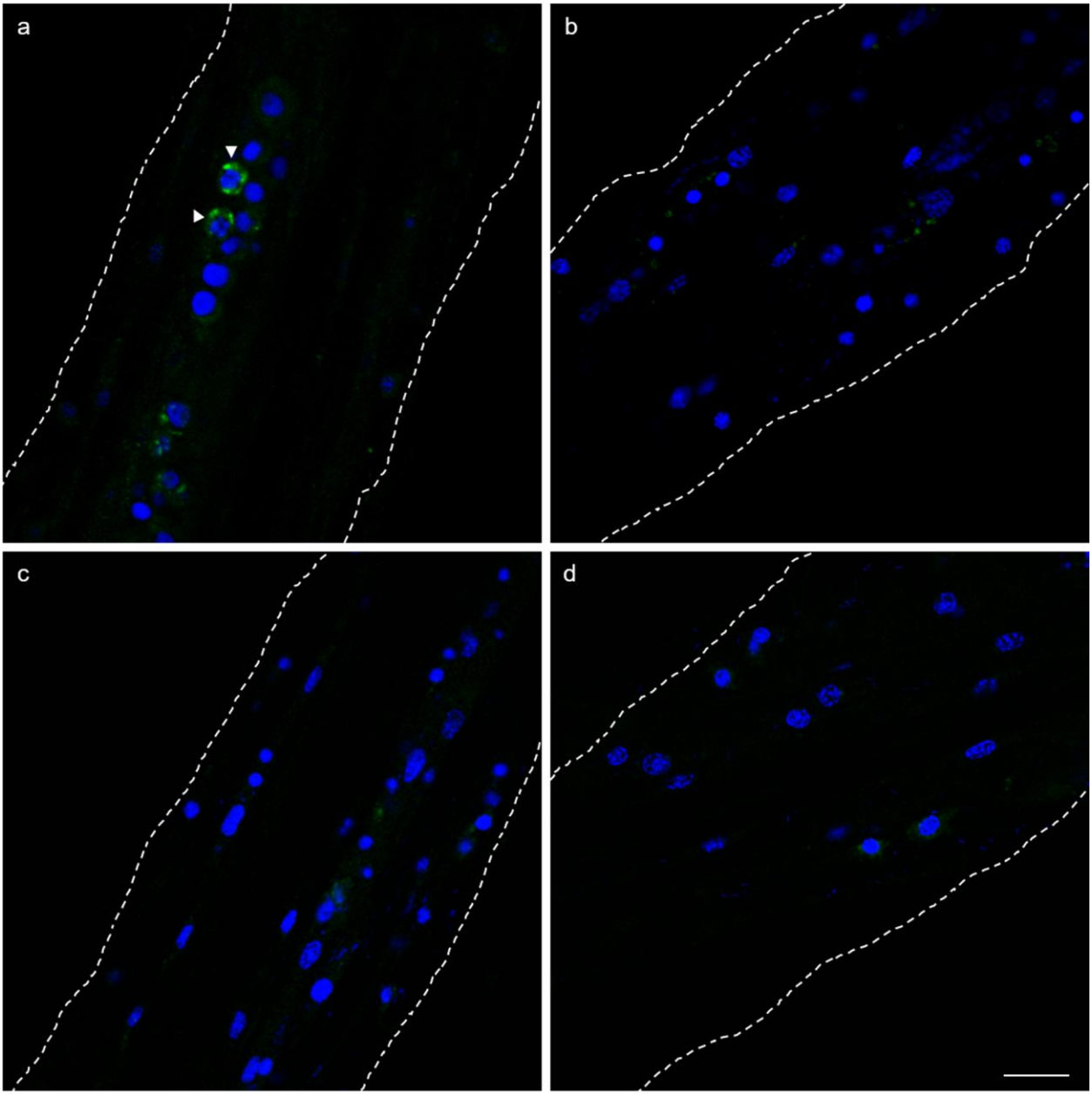

Figure 7

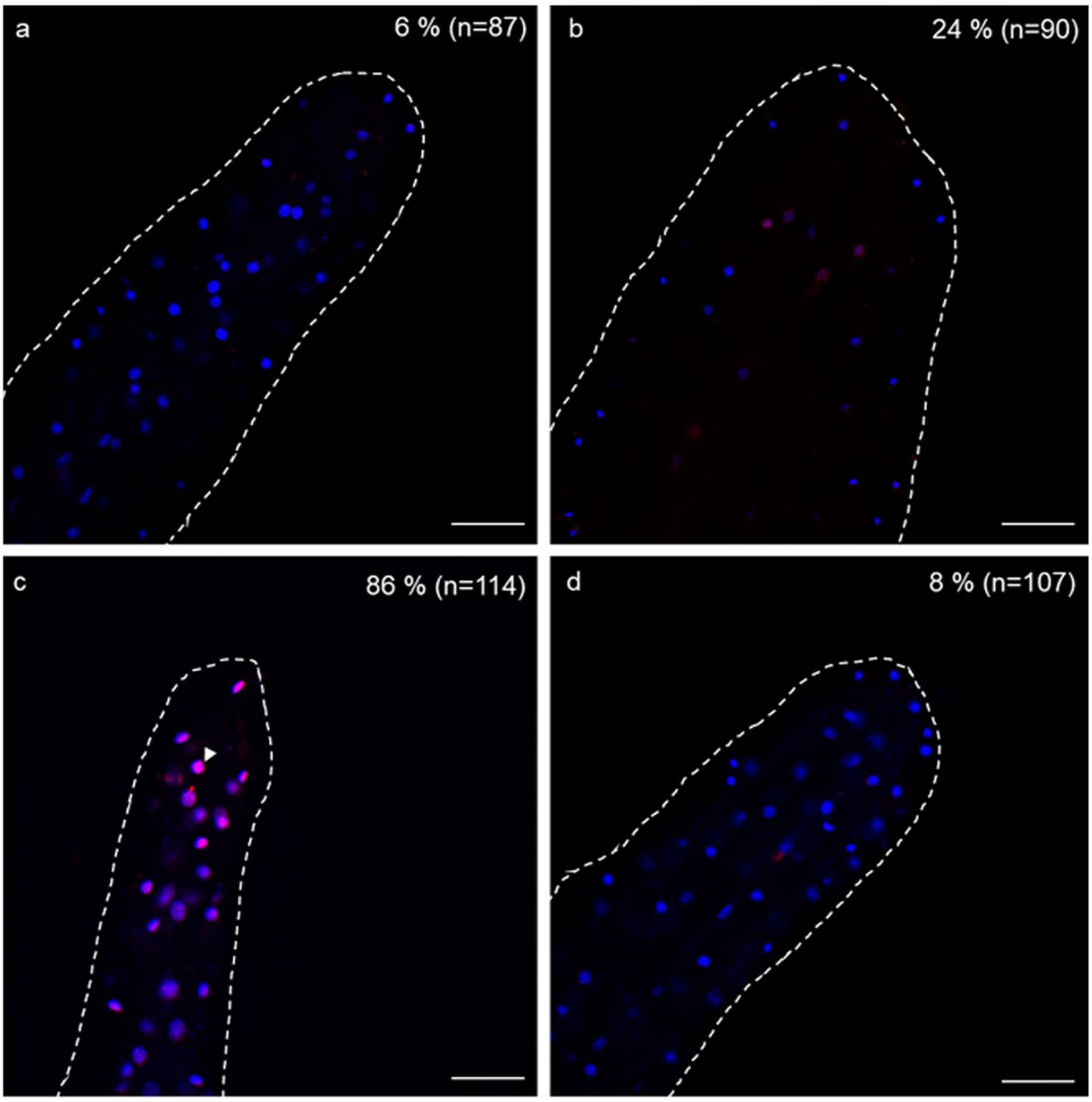
a
6 % (n=87)
b
24 % (n=90)
c
86 % (n=114)
d
8 % (n=107)

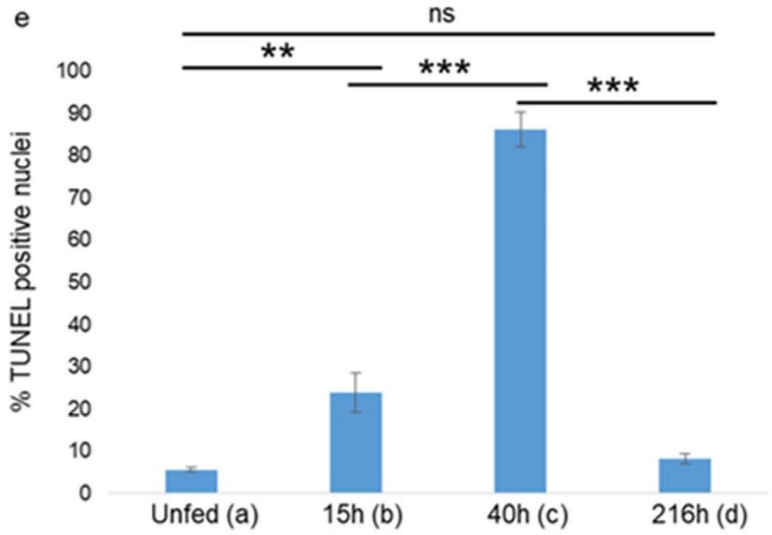
e
ns
**
***
***
% TUNEL positive nuclei
100
90
80
70
60
50
40
30
20
10
0
Unfed (a)
15h (b)
40h (c)
216h (d)

Figure 8

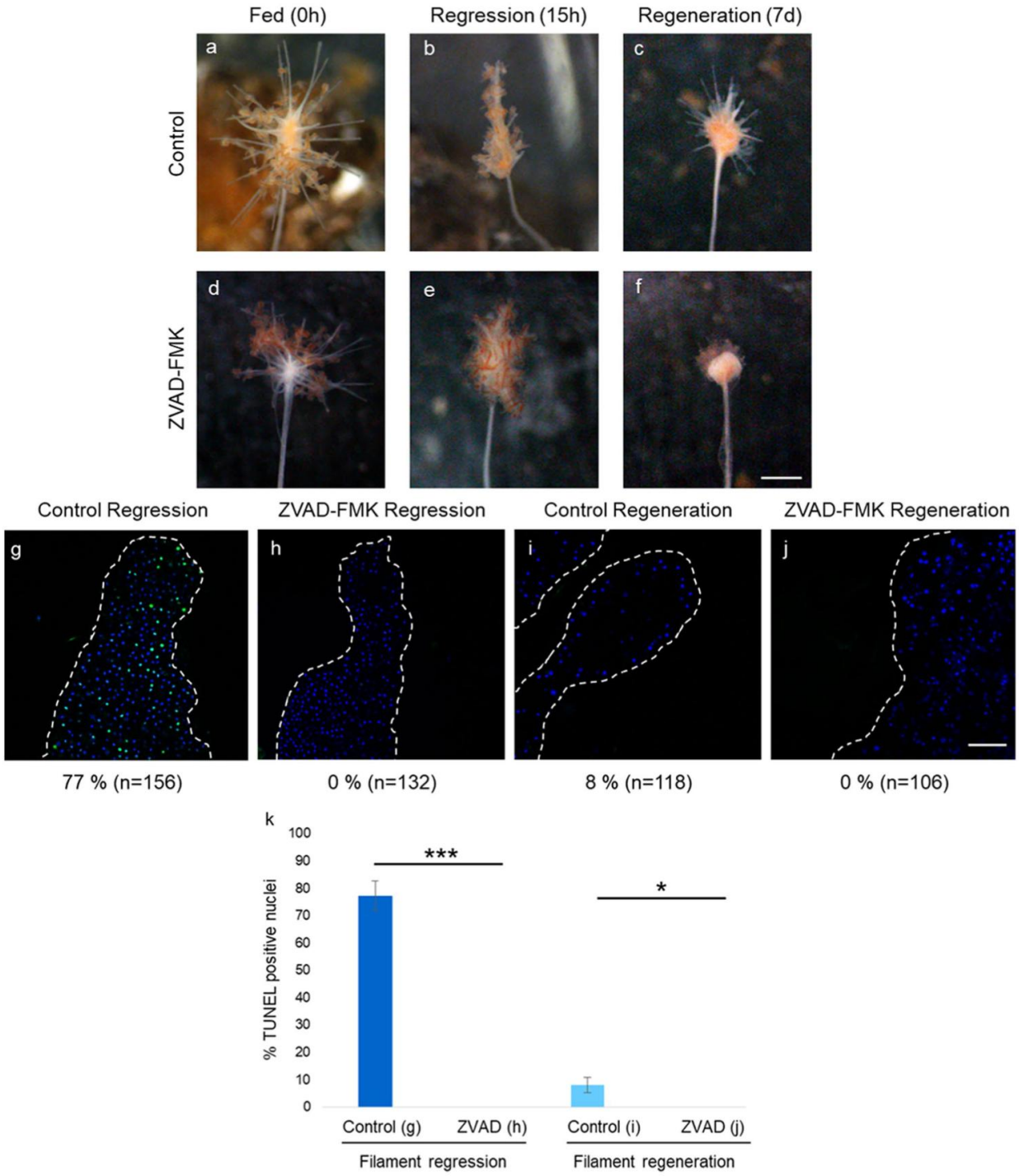
Fed (0h)
Regression (15h)
Regeneration (7d)
Control
ZVAD-FMK
a
b
c
d
e
f
Control Regression
ZVAD-FMK Regression
Control Regeneration
ZVAD-FMK Regeneration
g
h
i
j
77 % (n=156)
0 % (n=132)
8 % (n=118)
0 % (n=106)
k
% TUNEL positive nuclei
100
90
80
70
60
50
40
30
20
10
0
***
*
Control (g)
ZVAD (h)
Control (i)
ZVAD (j)
Filament regression
Filament regeneration

Figure 9